Table 4. Mean gas holdup data for runs with catalyst A.

Run No.	U_G (m/s)	Gas Type	C to N2 L/D = 5.4	N2 to D L/D = 11.1	D to N1 L/D = 17.8	N1 to E L/D = 24.5
R13.1	0.26	Texaco	44.7%	42.4%	44.9%	52.8%
R13.2	0.15	Kingsport	34.5%	31.6%	33.8%	41.3%
R13.3	0.34	Kingsport	43.7%	41.1%	43.0%	50.2%

Table 5. Mean gas holdup data for runs with catalyst B.

Run No.	U_G (m/s)	Gas Type	C to N2 L/D = 5.4	N2 to D L/D = 11.1	D to N1 L/D = 17.8	N1 to E L/D = 24.5
R14.4	0.14	Texaco	32.1%	29.0%	32.2%	38.7%
R14.1	0.26	Texaco	37.7%	34.7%	37.7%	44.2%
R14.5	0.25	Texaco	38.2%	35.5%	38.5%	46.4%
R14.9	0.046	Kingsport	16.3%	11.4%	12.5%	
R14.2	0.15	Kingsport	28.8%	24.7%	27.0%	32.8%
R14.3	0.36	Kingsport	36.0%	32.8%	34.4%	41.1%

Table 6. Standard deviations in gas holdup data for runs with catalyst A.

Run No.	U_G (m/s)	Gas Type	C to N2 L/D = 5.4	N2 to D L/D = 11.1	D to N1 L/D = 17.8	N1 to E L/D = 24.5
R13.1	0.26	Texaco	0.65%	0.59%	0.49%	1.06%
R13.2	0.15	Kingsport	0.57%	0.45%	0.32%	0.89%
R13.3	0.34	Kingsport	0.93%	0.88%	0.71%	1.53%

Table 7. Standard deviations in gas holdup data for runs with catalyst B.

Run No.	U_G (m/s)	Gas Type	C to N2 L/D = 5.4	N2 to D L/D = 11.1	D to N1 L/D = 17.8	N1 to E L/D = 24.5
R14.4	0.14	Texaco	0.46%	0.38%	0.35%	1.04%
R14.1	0.26	Texaco	0.75%	0.71%	0.64%	1.30%
R14.5	0.25	Texaco	0.77%	0.71%	0.65%	1.29%
R14.9	0.046	Kingsport	0.32%	0.23%	0.31%	0.48%
R14.2	0.15	Kingsport	0.51%	0.44%	0.39%	0.84%
R14.3	0.36	Kingsport	1.05%	1.04%	0.88%	1.85%

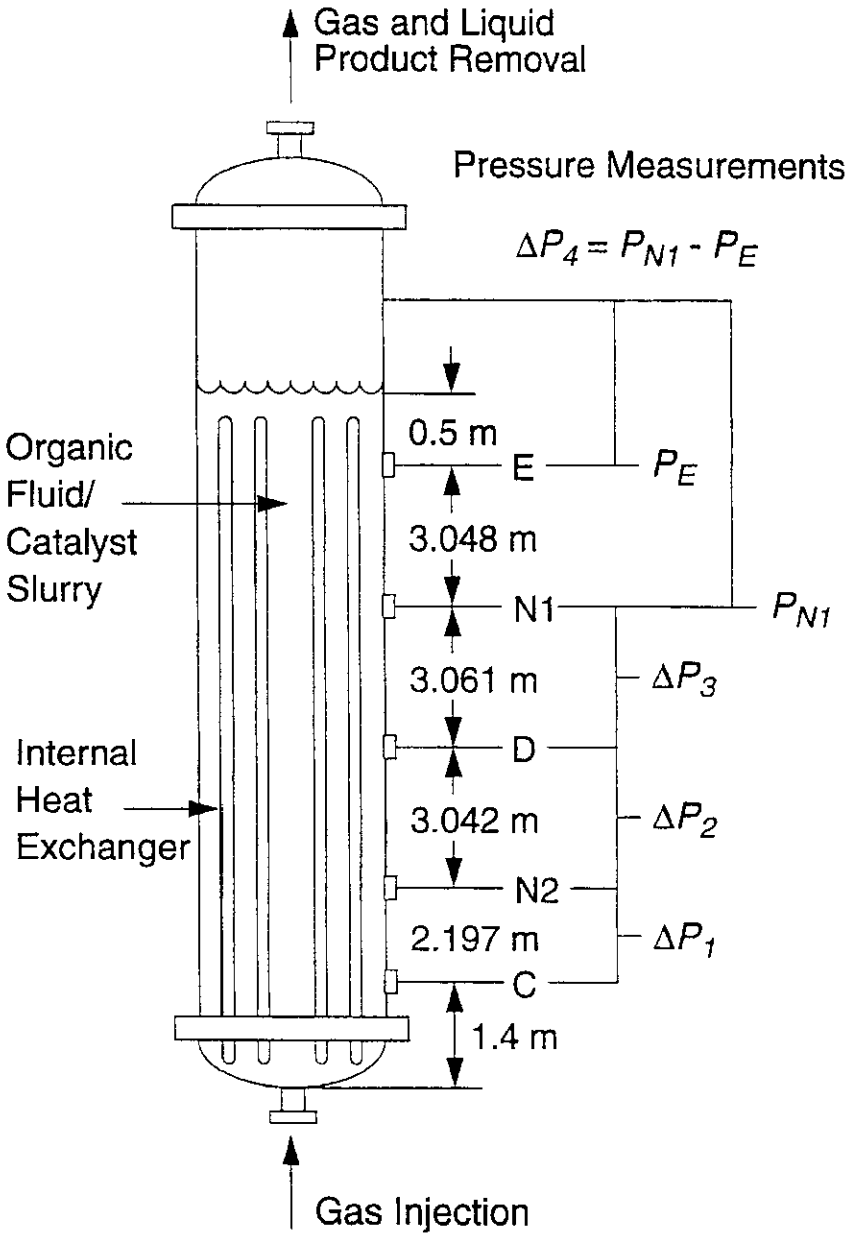

Figure 1. Schematic diagram of LaPorte Alternative Fuels Development Unit (AFDU); 18 in. (0.457 m) inside diameter, 50 ft. (15.24 m) normal liquid level during operation, 2000 psig (13.8 MPa) design pressure, 700 °F (371 °C) design temperature.

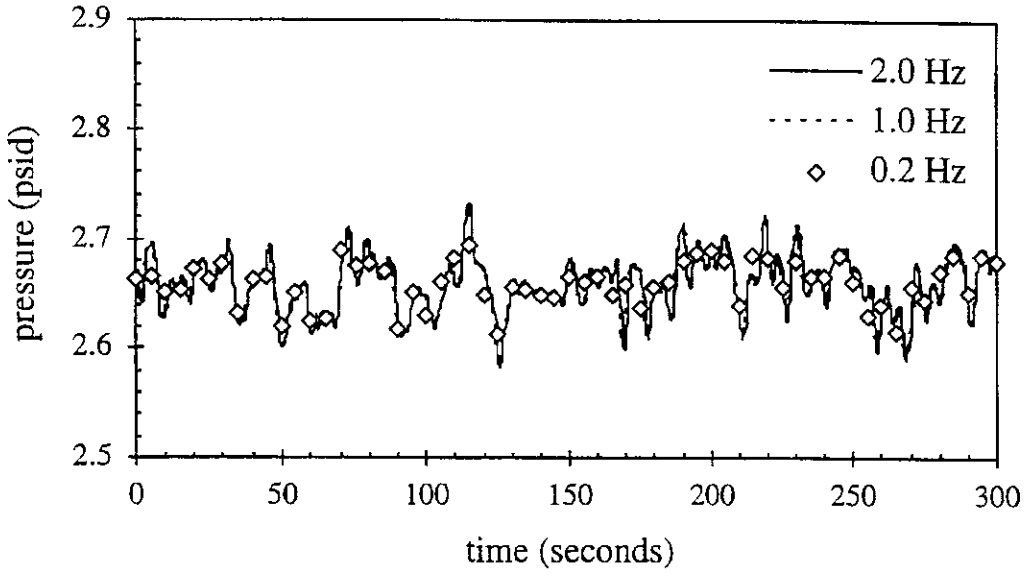

Figure 2. Time trace of differential pressure signal between nozzles N2 and D (L/D = 11.1) at different sampling rates for Run No. R13.1, U_G = 0.26 m/s, Texaco gas, ω_S = 49%, 765 psia (5.27 MPa), 482 °F (250 °C).

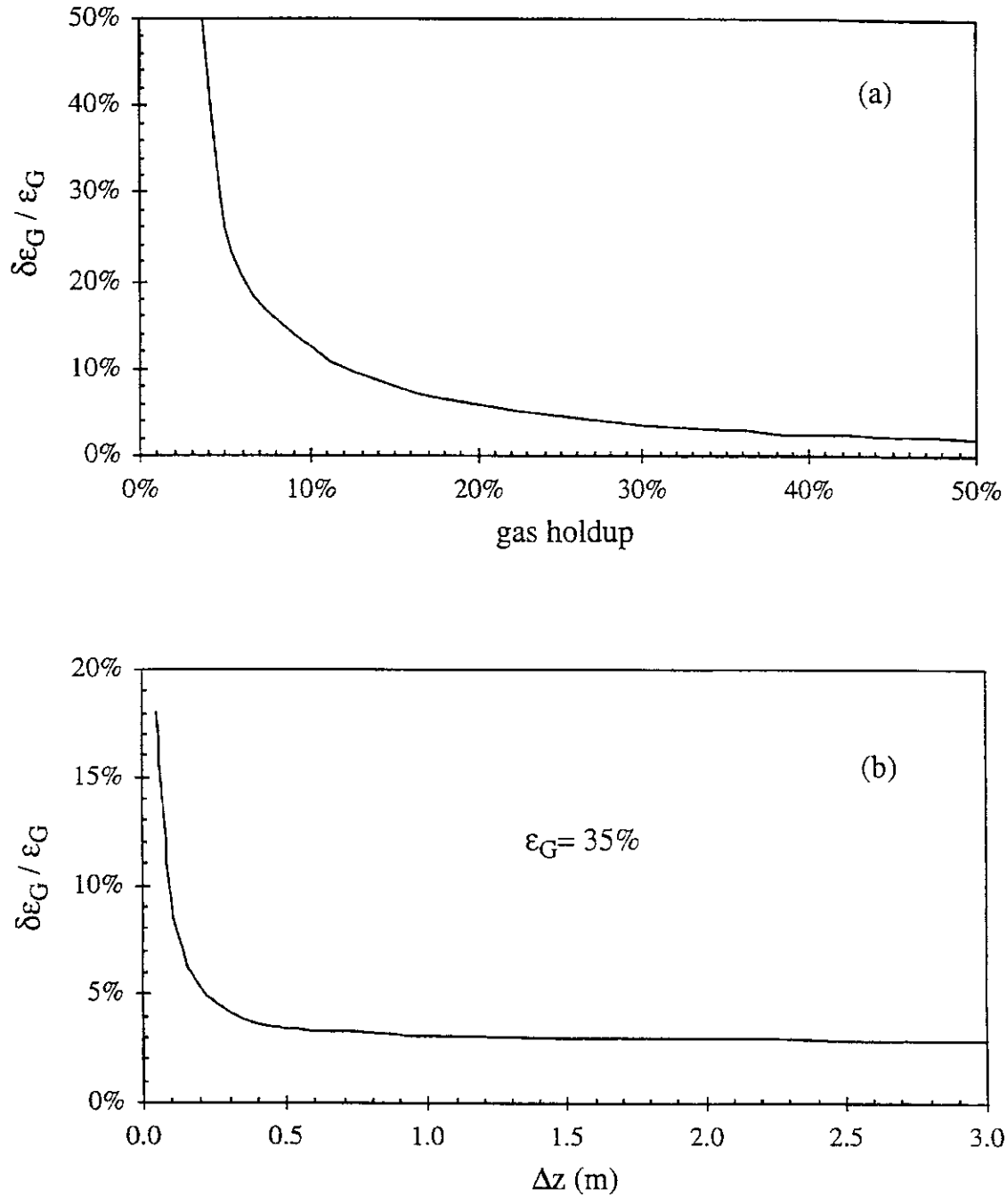

Figure 3. Relative uncertainty in gas holdup ($\delta\varepsilon_G/\varepsilon_G$) as function of (a) gas holdup and (b) distance between pressure taps under AFDU operating conditions, Texaco gas, and catalyst A.

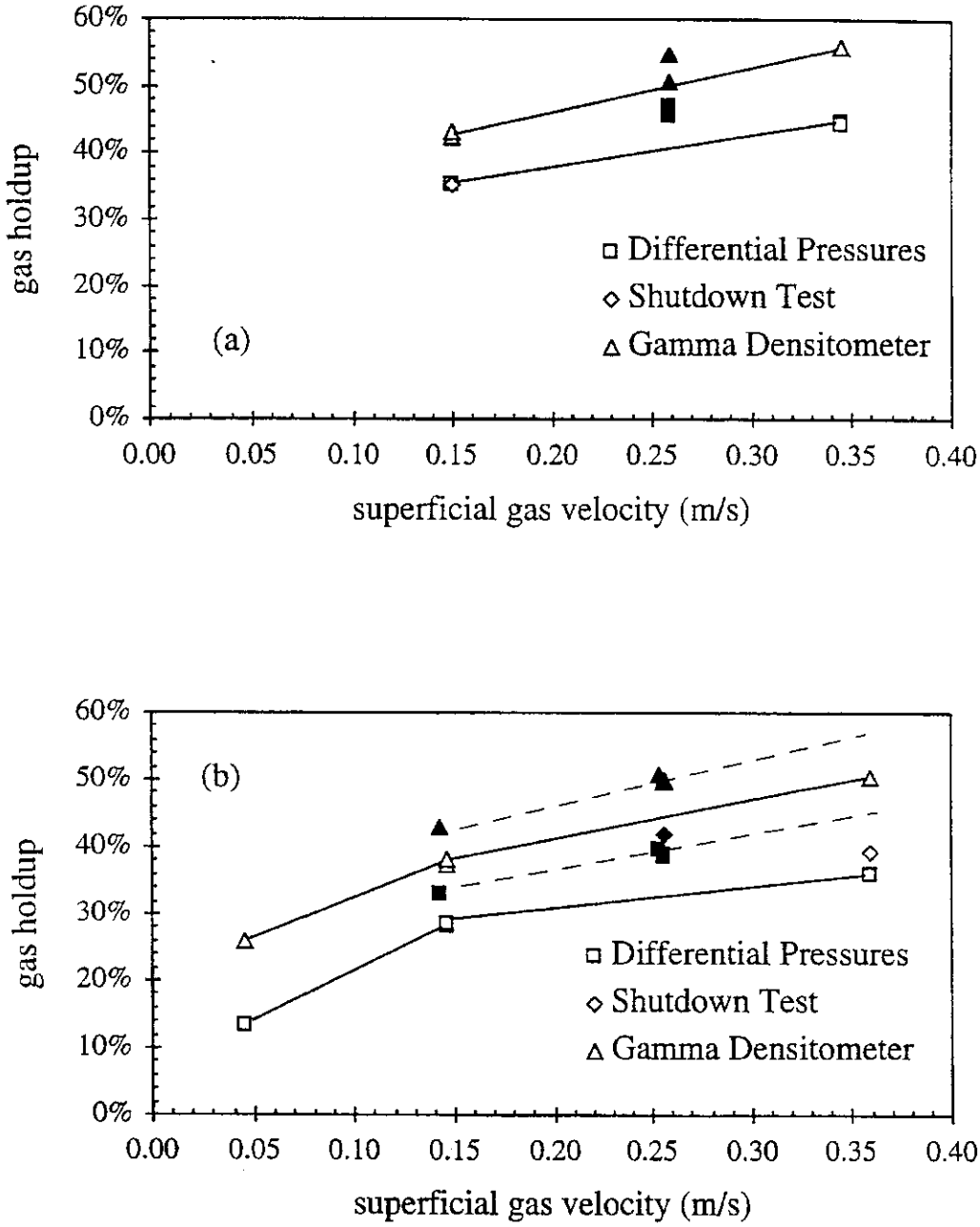

Figure 4. Comparison of gas holdups measured using differential pressures, gamma densitometer and shutdown test for (a) catalyst A runs (R13) and (b) catalyst B runs (R14); closed and open symbols denote Texaco and Kingsport gas, ω_S = 39%-49%, 535-765 psia (3.69-5.27 MPa), 482 °F (250 °C).

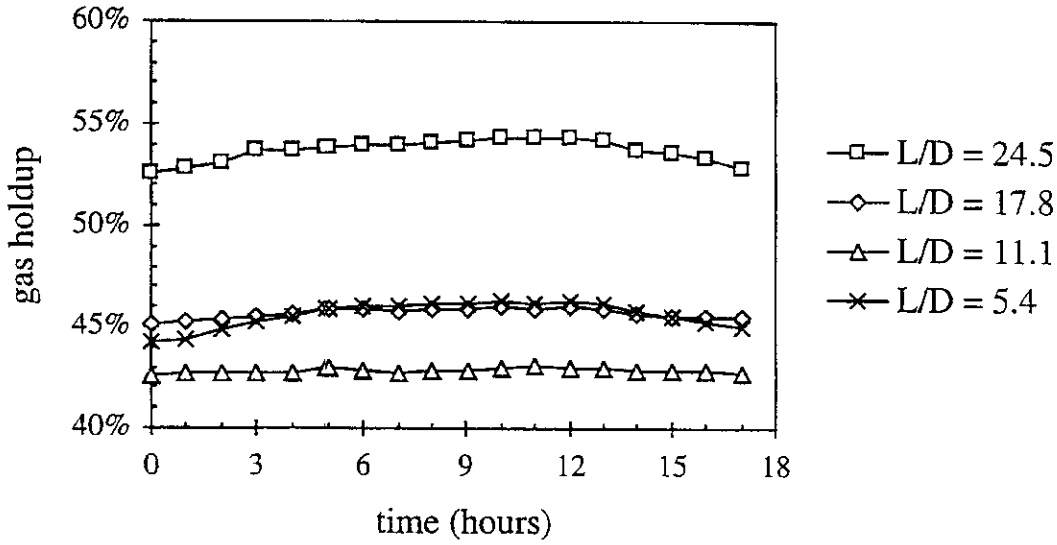

Figure 5. Gas holdups averaged over one-hour periods for catalyst A run number R13.1; U_G = 0.26 m/s, Texaco gas, ω_S = 49%, 765 psia (5.27 MPa), 482 °F (250 °C).

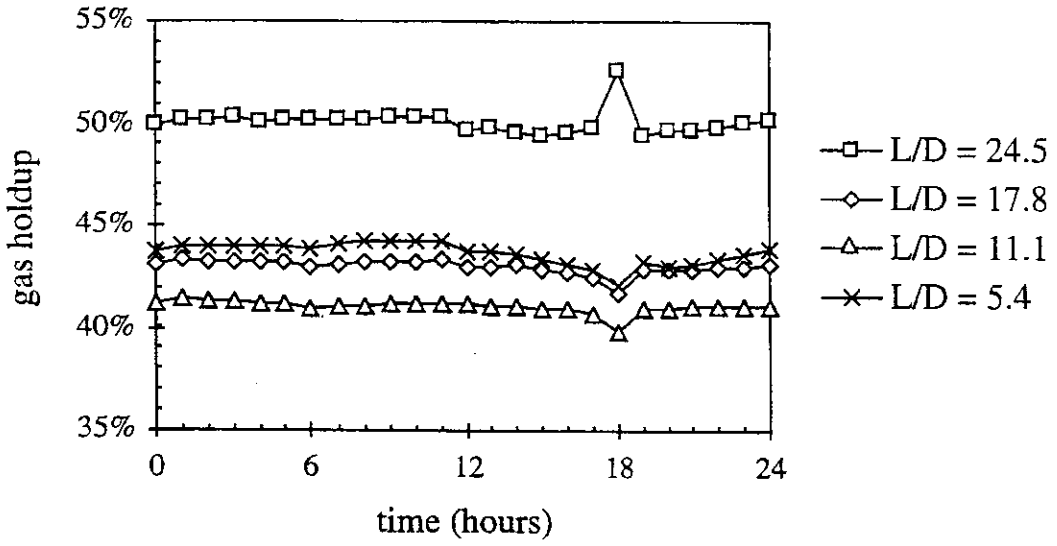

Figure 6. Gas holdups averaged over one-hour periods for catalyst A run number R13.3; U_G = 0.34 m/s, Kingsport gas,, ω_S = 48%, 735 psia (5.07 MPa), 482 °F (250 °C).

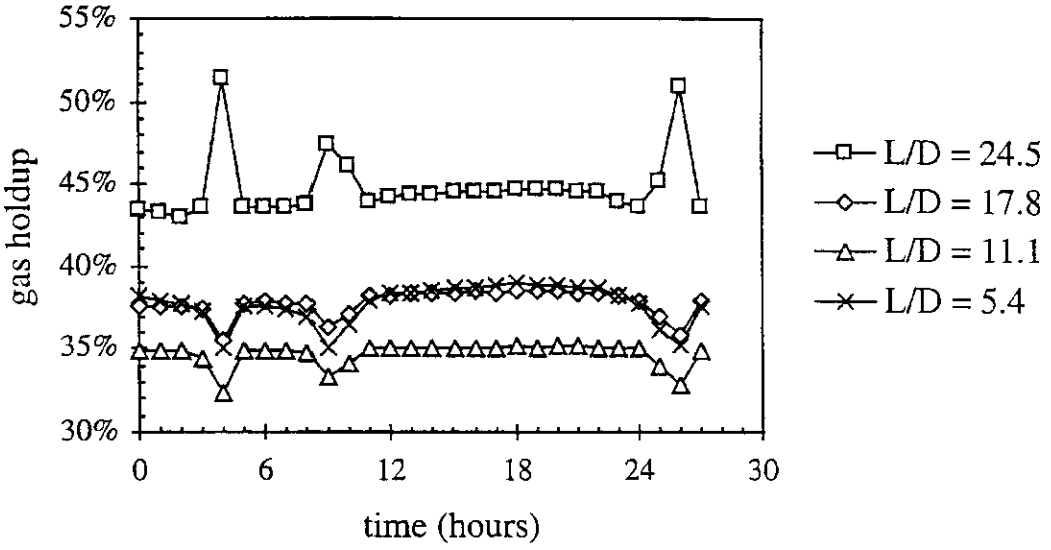

Figure 7. Gas holdups averaged over one-hour periods for catalyst B run number R14.1; U_G = 0.26 m/s, Texaco gas, ω_S = 44%, 765 psia (5.27 MPa), 482 °F (250 °C).

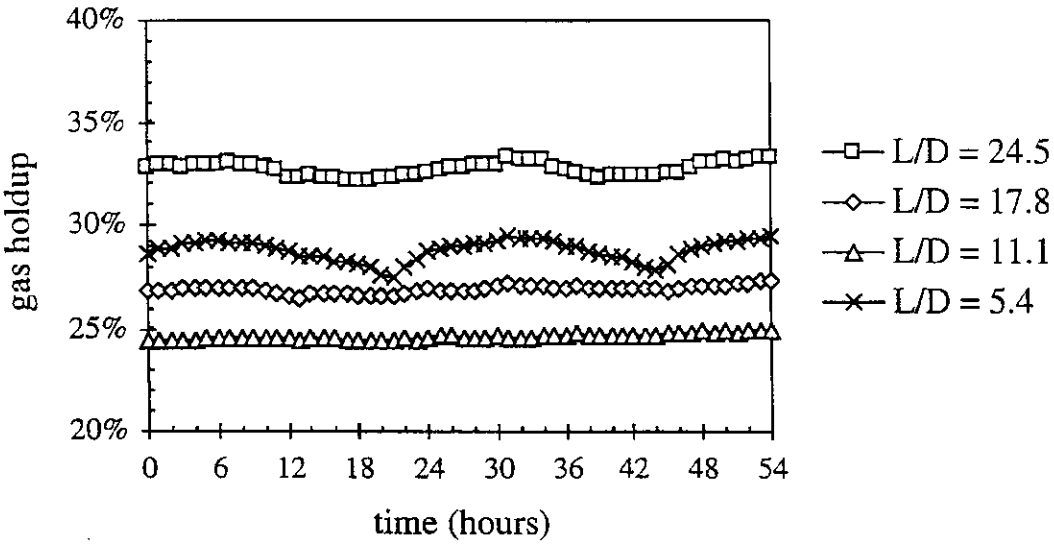

Figure 8. Gas holdups averaged over one-hour periods for catalyst B run number R14.2; U_G = 0.15 m/s, Kingsport gas, ω_S = 39%, 750 psia (5.17 MPa), 482 °F (250 °C).

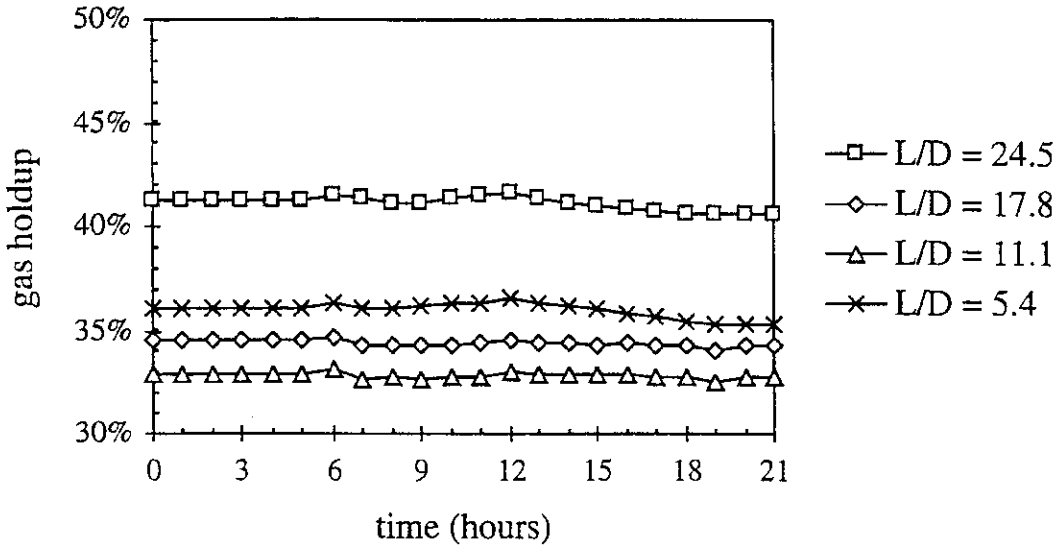

Figure 9. Gas holdups averaged over one-hour periods for catalyst B run number R14.3; U_G = 0.36 m/s, Kingsport gas, ω_S = 42%, 535 psia (3.69 MPa), 482 °F (250 °C).

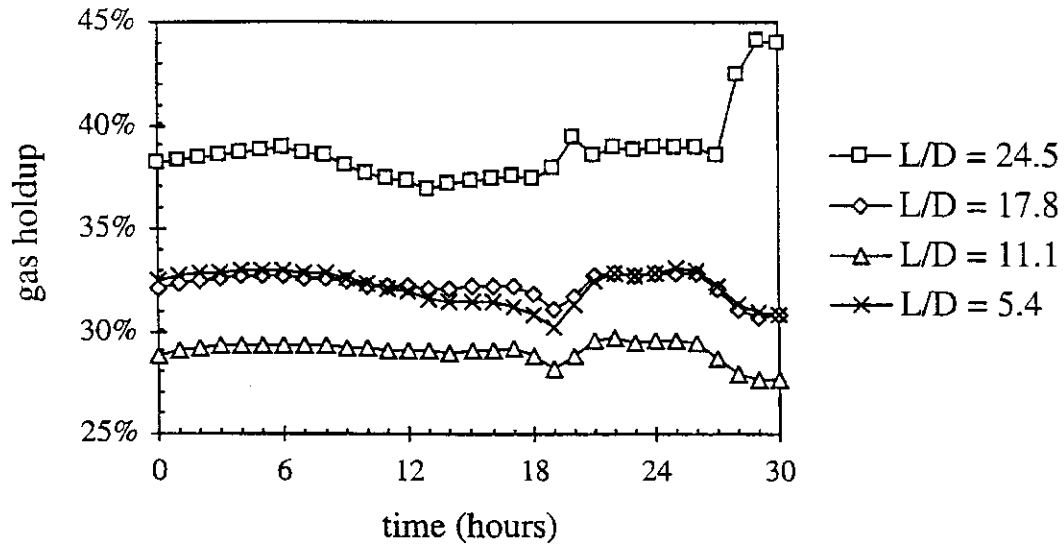

Figure 10. Gas holdups averaged over one-hour periods for catalyst B run number R14.4; U_G = 0.14 m/s, Texaco gas, ω_S = 41%, 765 psia (5.27 MPa), 482 °F (250 °C).

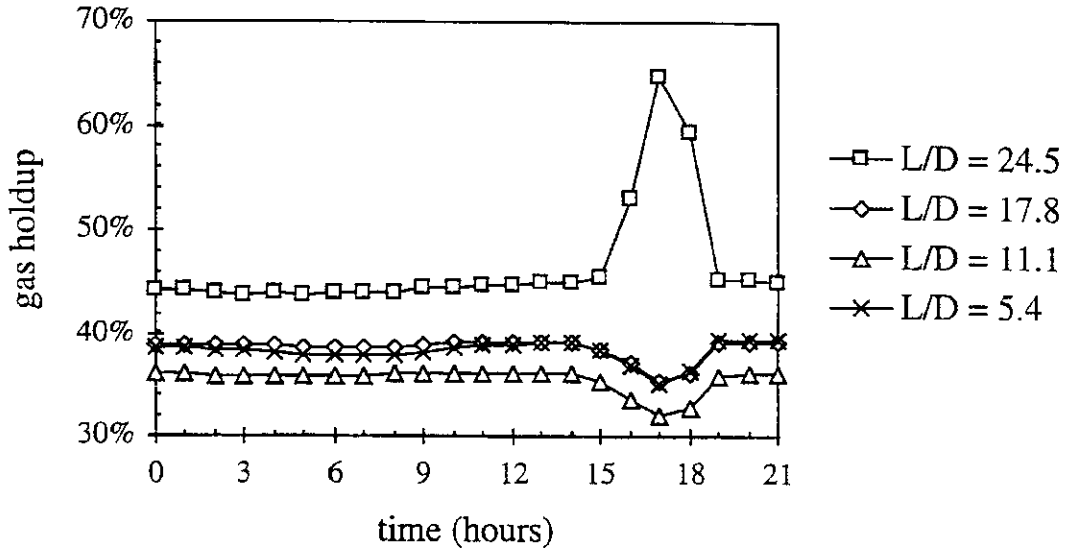

Figure 11. Gas holdups averaged over one-hour periods for catalyst B run number R14.5; U_G = 0.25 m/s, Texaco gas, ω_S = 45%, 765 psia (5.27 MPa), 482 °F (250 °C).

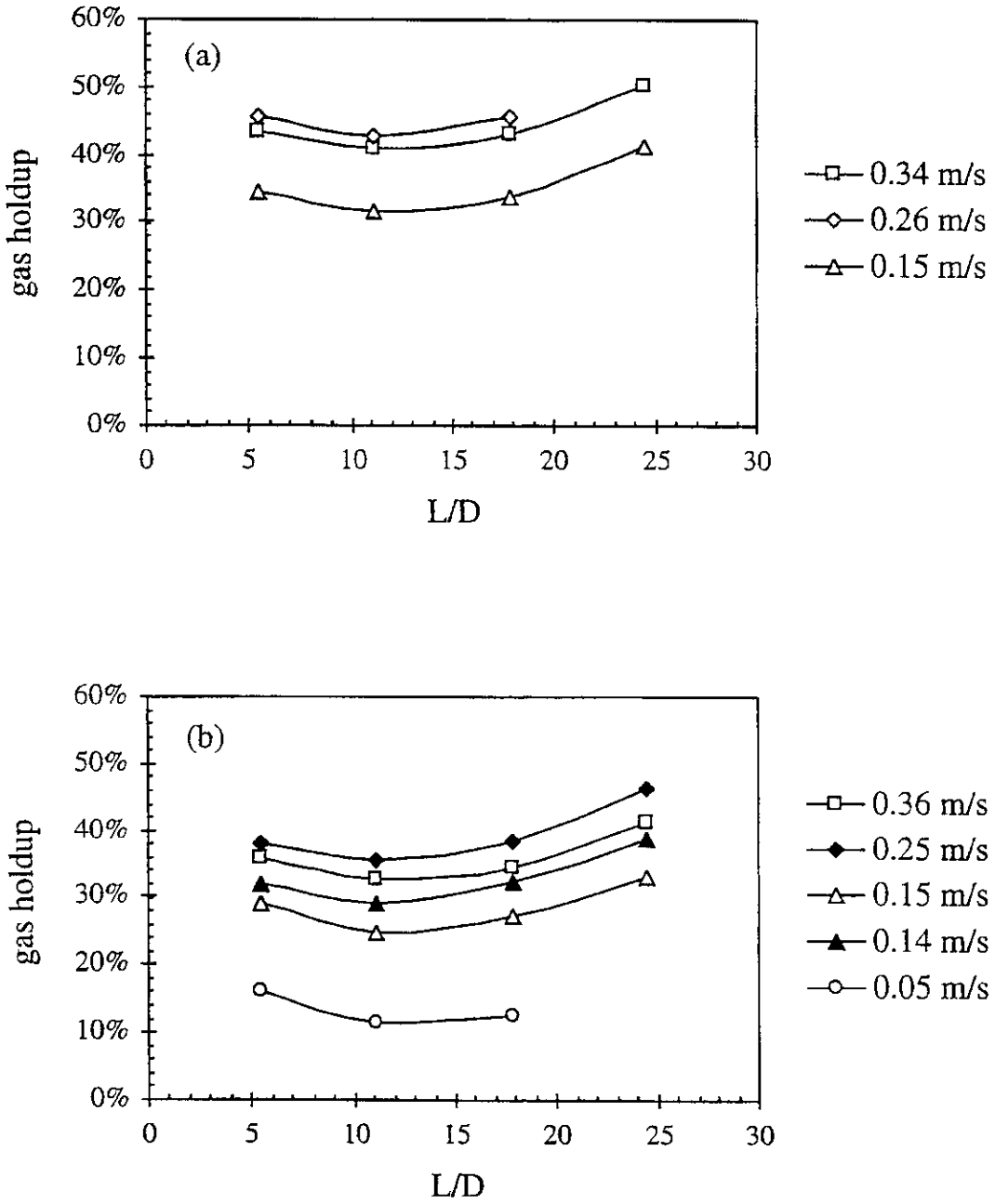

Figure 12. Gas holdup versus axial distance from sparger and superficial gas velocity in the AFDU for (a) catalyst A and (b) catalyst B; closed and open symbols denote Texaco and Kingsport gas, ω_S = 39-44%, 535-765 psia (3.69-5.27 MPa), 482 °F (250 °C).

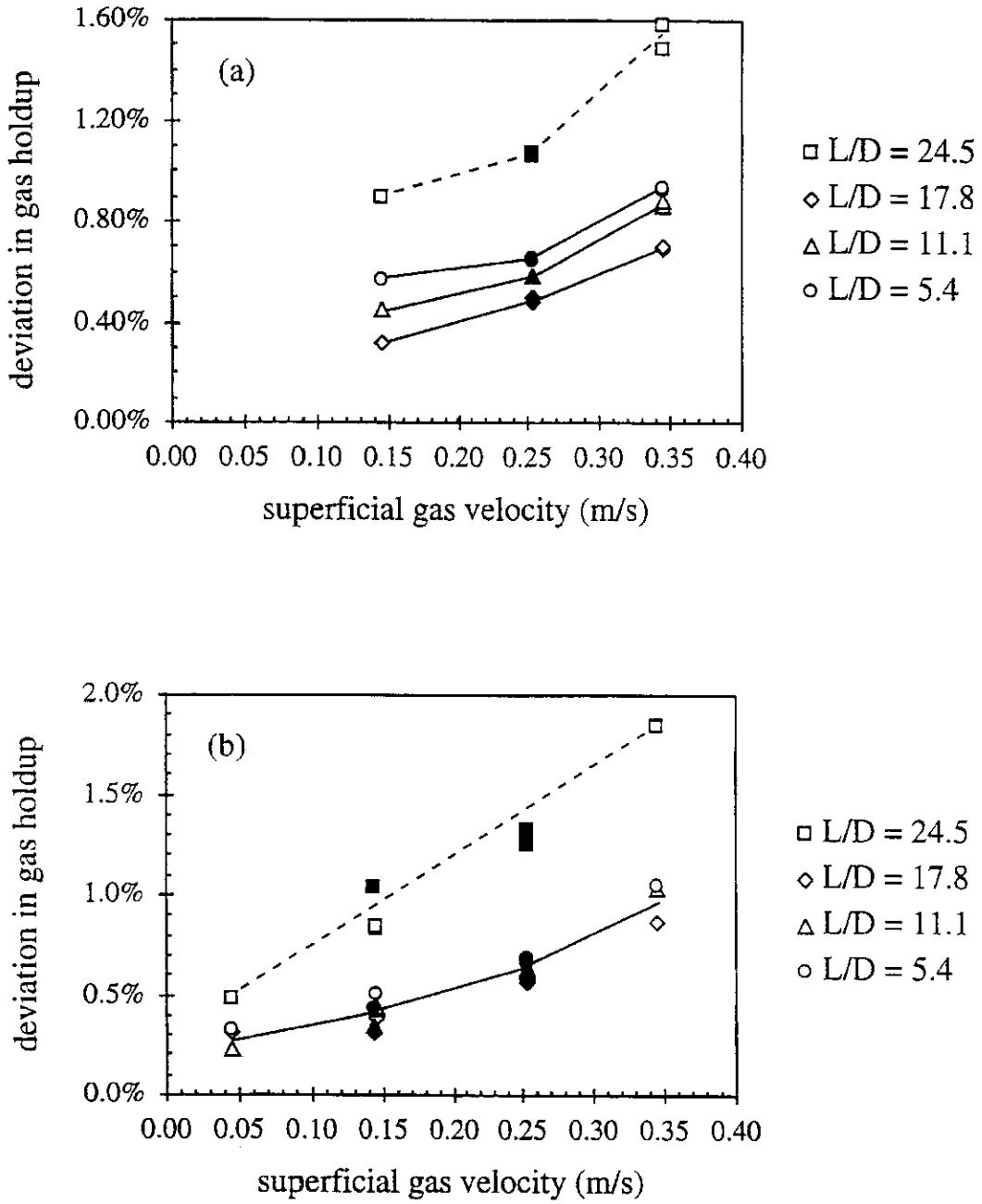

Figure 13. Standard deviation of gas holdup versus superficial gas velocity and axial distance from sparger in the AFDU for (a) catalyst A and (b) catalyst B; closed and open symbols denote Texaco and Kingsport gas, ω_S = 39-44%, 535-765 psia (3.69-5.27 MPa), 482 °F (250 °C).

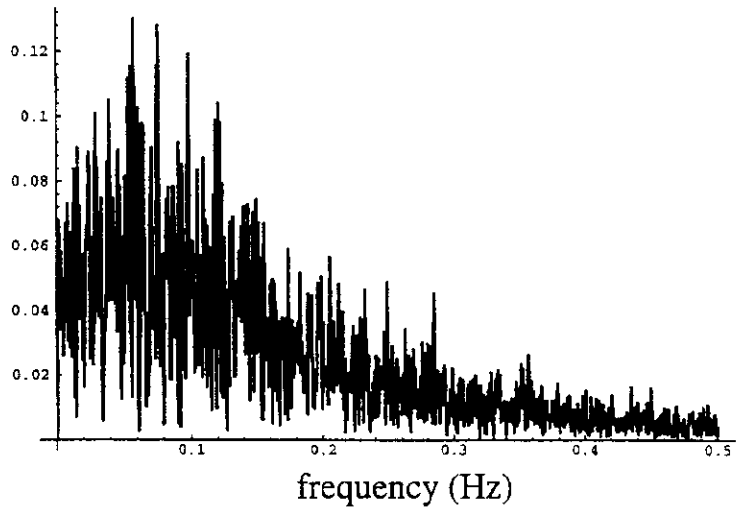

Figure 14. Frequency spectrum of differential pressure for catalyst B run number R14.3; U_G = 0.36 m/s, Kingsport gas; ω_S = 42%, 535 psia (3.69 MPa), 482 °F (250 °C).

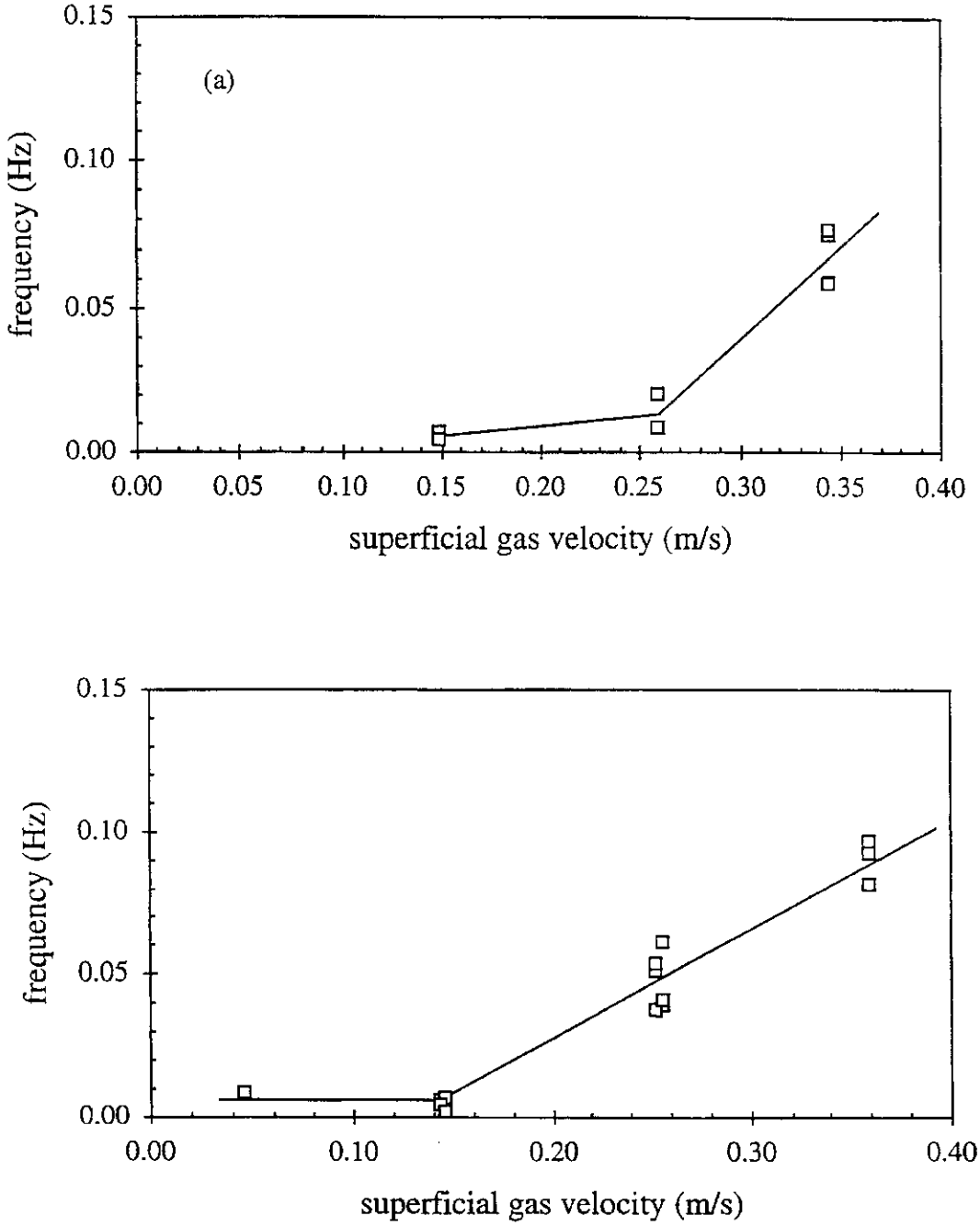

Figure 15. Dominant frequency component from Fourier analysis of differential pressures versus superficial gas velocity in the AFDU for (a) catalyst A and (b) catalyst B; ω_S = 39-44%, 535-765 psia (3.69-5.27 MPa), 482 °F (250 °C).

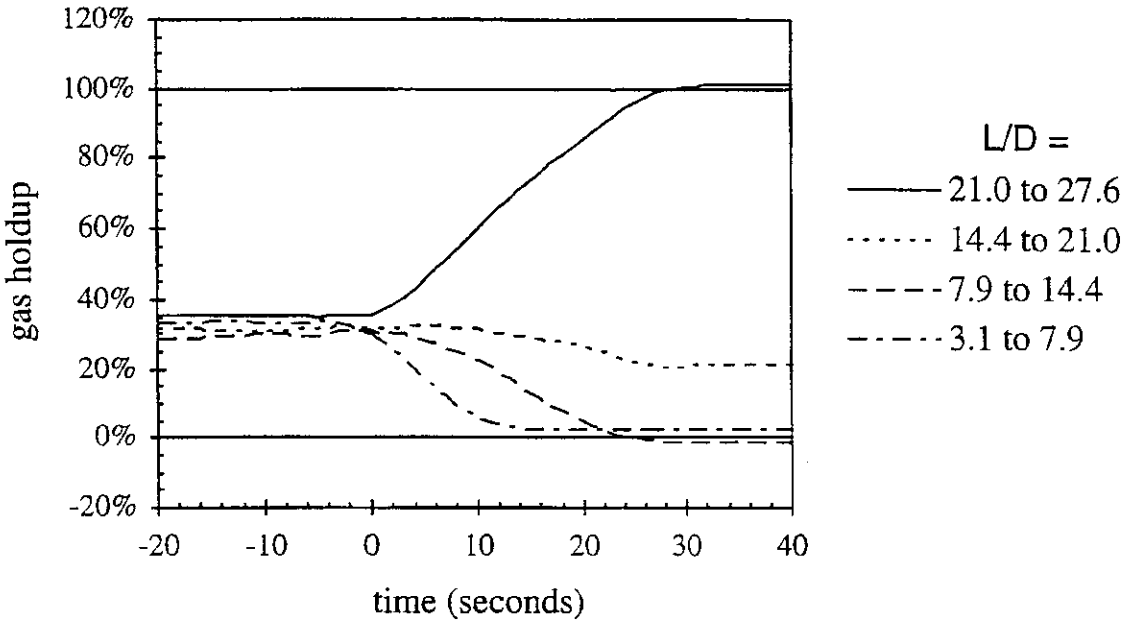

Figure 16. Dynamic Gas Disengagement curves from differential pressure measurements in AFDU for Run No. R13.2; $U_G = 0.15$ m/s, Kingsport gas, $\omega_S = 43\%$, catalyst A, 750 psia (5.17 MPa) and 482 °F (250 °C).

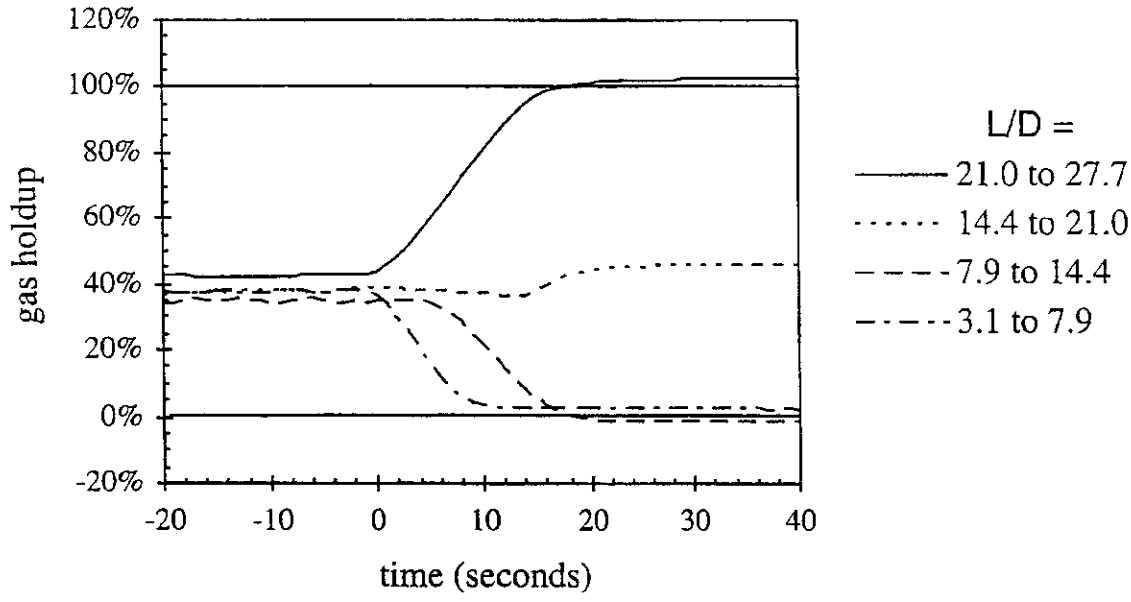

Figure 17. Dynamic Gas Disengagement curves from differential pressure measurements in AFDU for Run No. R14.1; $U_G = 0.25$ m/s, Texaco gas, $\omega_S = 43\%$, catalyst B, 765 psia (5.27 MPa) and 482 °F (250 °C).

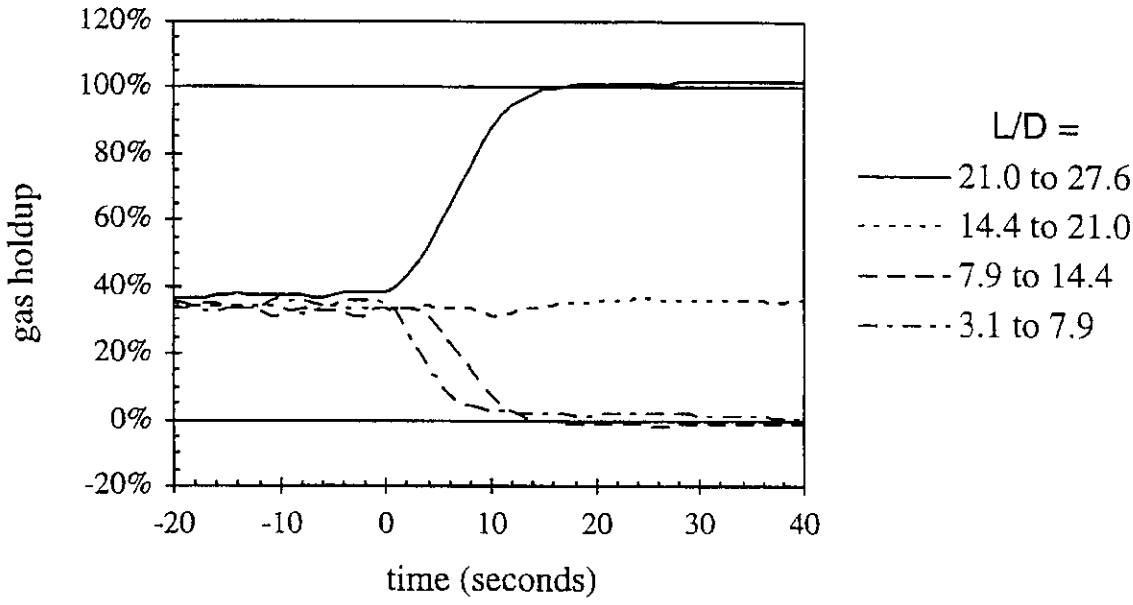

Figure 18. Dynamic Gas Disengagement curves from differential pressure measurements in AFDU for Run No. R14.3; $U_G = 0.36$ m/s, Kingsport gas, $\omega_S = 43\%$, 535 psia (3.69 MPa) and 482 °F (250 °C).

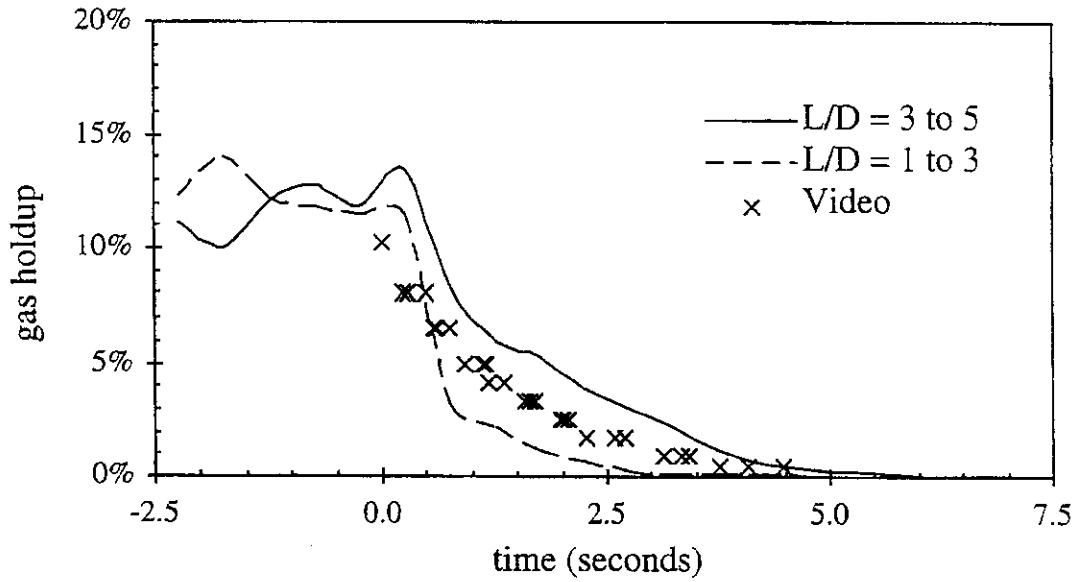

Figure 19. Dynamic Gas Disengagement curves from differential pressure measurements and high-speed video in 0.19 m Lexan column with air, water and 80 micron glass beads at atmospheric pressure and temperature; $U_G = 0.088$ m/s, $\omega_S = 40\%$.

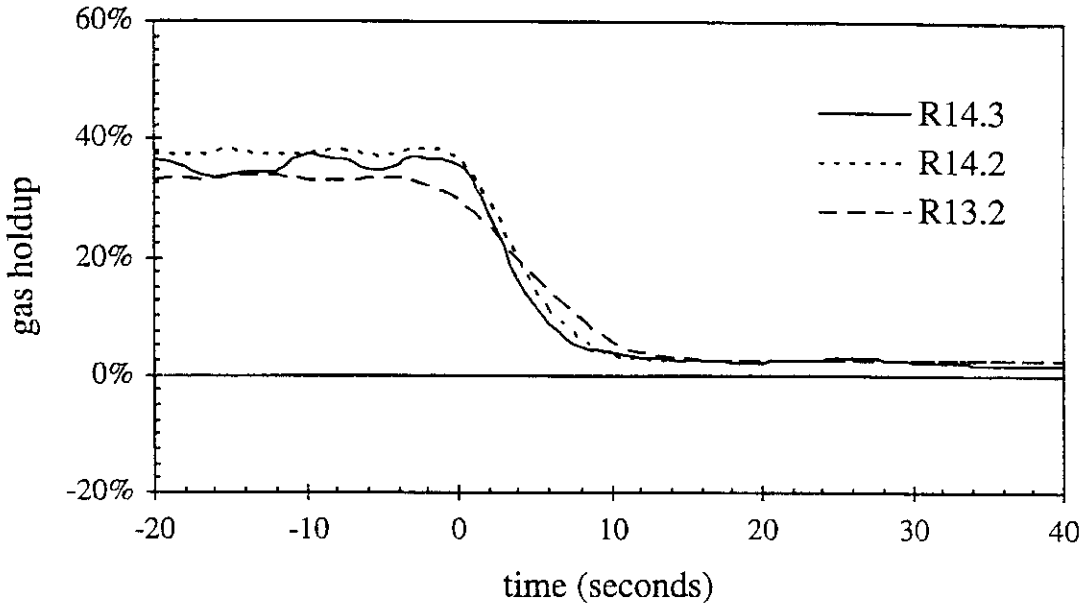

Figure 20. Dynamic Gas Disengagement curves in AFDU after run numbers R13.2, R14.1 and R14.3 at L/D between 3.1 and 7.9.

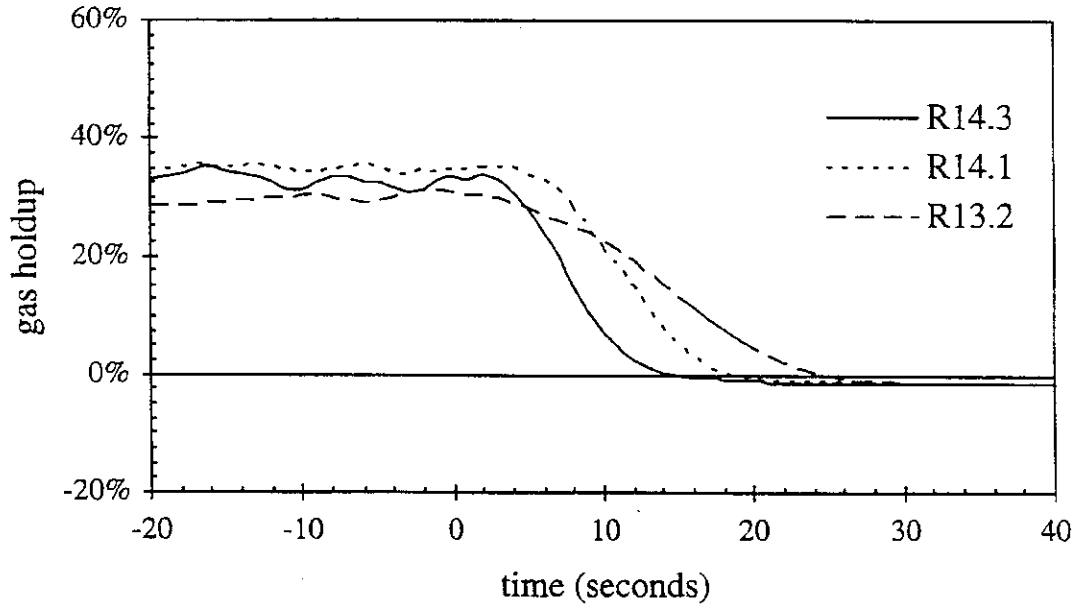

Figure 21. Dynamic Gas Disengagement curves in AFDU after run numbers R13.2, R14.1 and R14.3 at L/D between 7.9 and 14.4.

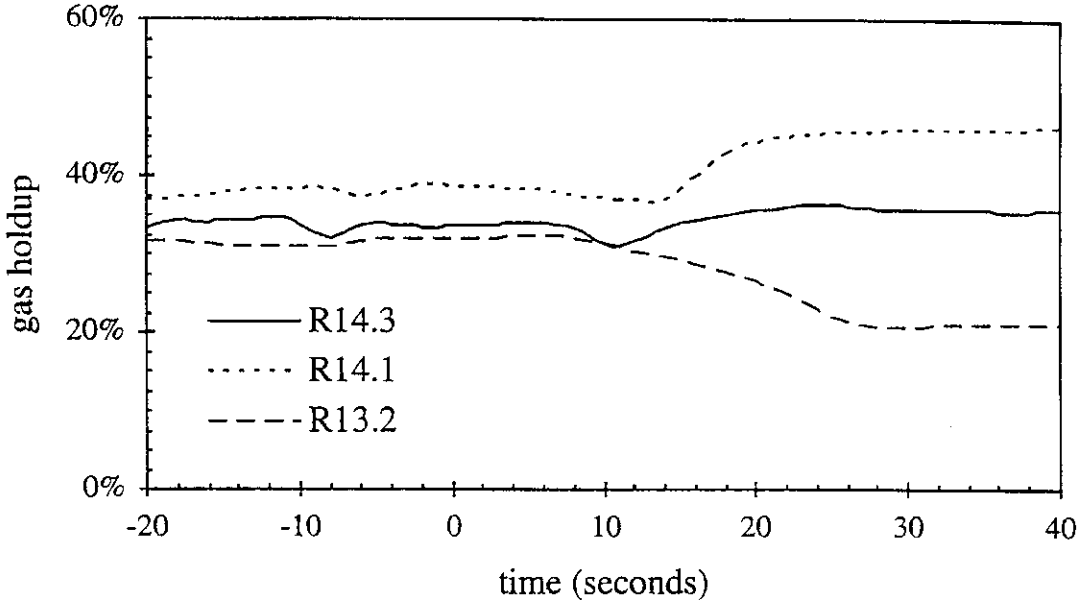

Figure 22. Dynamic Gas Disengagement curves in AFDU after run numbers R13.2, R14.1 and R14.3 at L/D between 14.4 and 21.0.

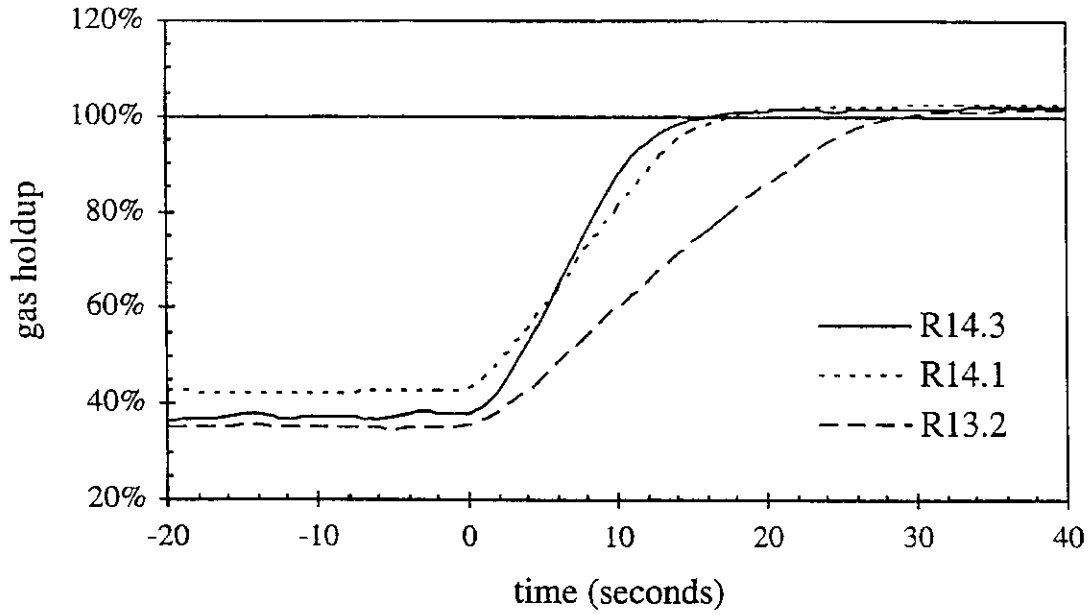

Figure 23. Dynamic Gas Disengagement curves in AFDU after run numbers R13.2, R14.1 and R14.3 at L/D between 21.0 and 27.6.

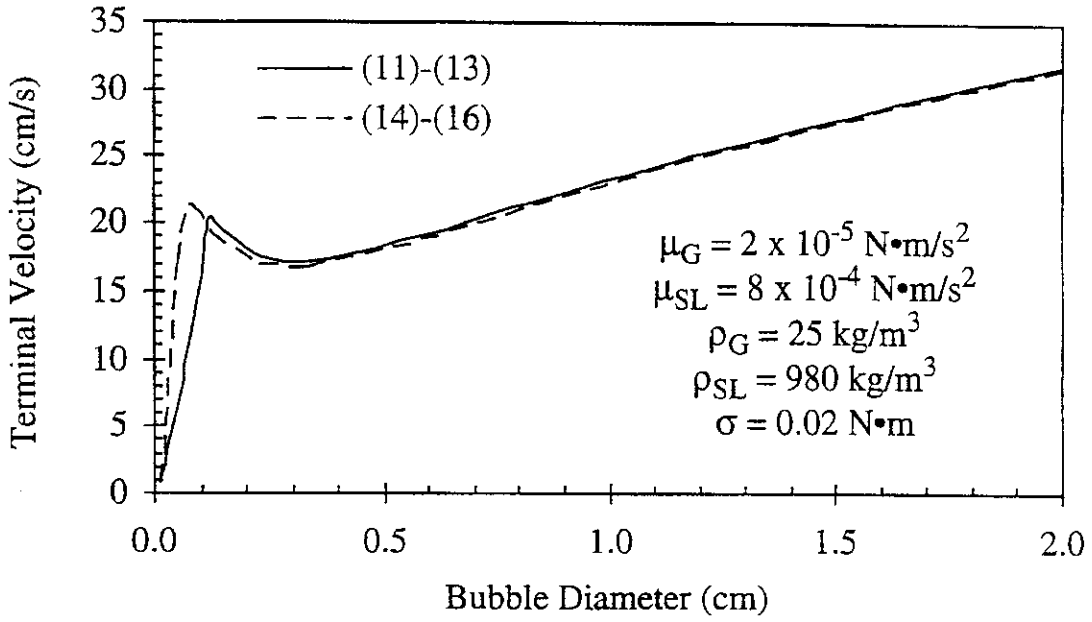

Figure 24. Comparison of terminal bubble velocity versus bubble diameter using (11)-(13) (Stokes' Law; Peebles and Garber, 1953; Clift et al., 1978) and (14)-(16) (a correlation by Jamialahmadi, 1994).

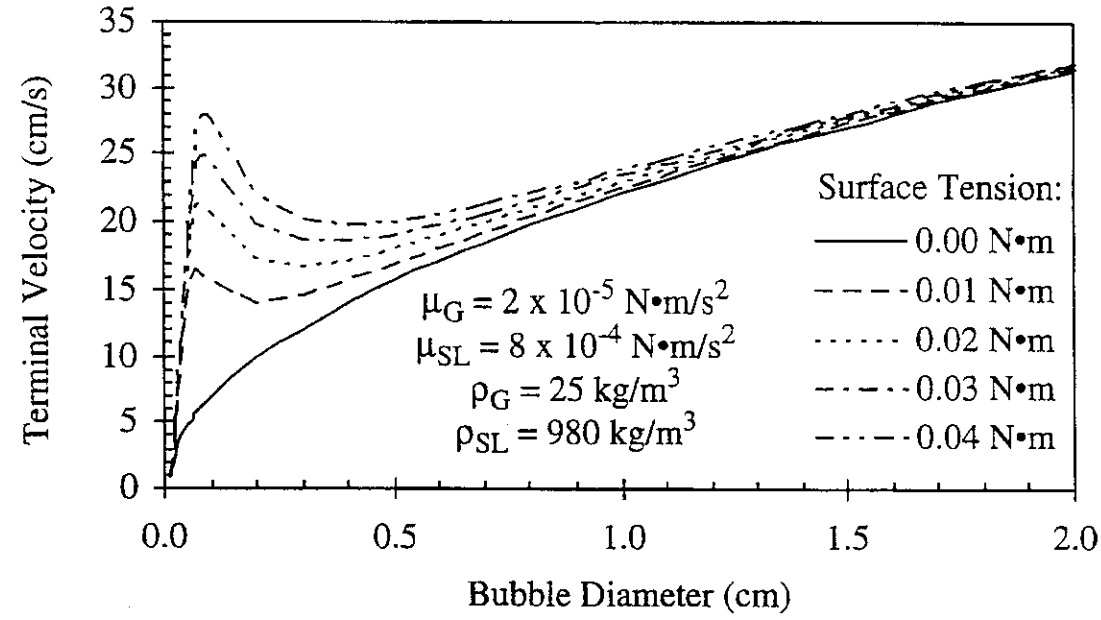

Figure 25. Terminal bubble velocity versus bubble diameter and surface tension using correlation by Jamialahmadi (1994).

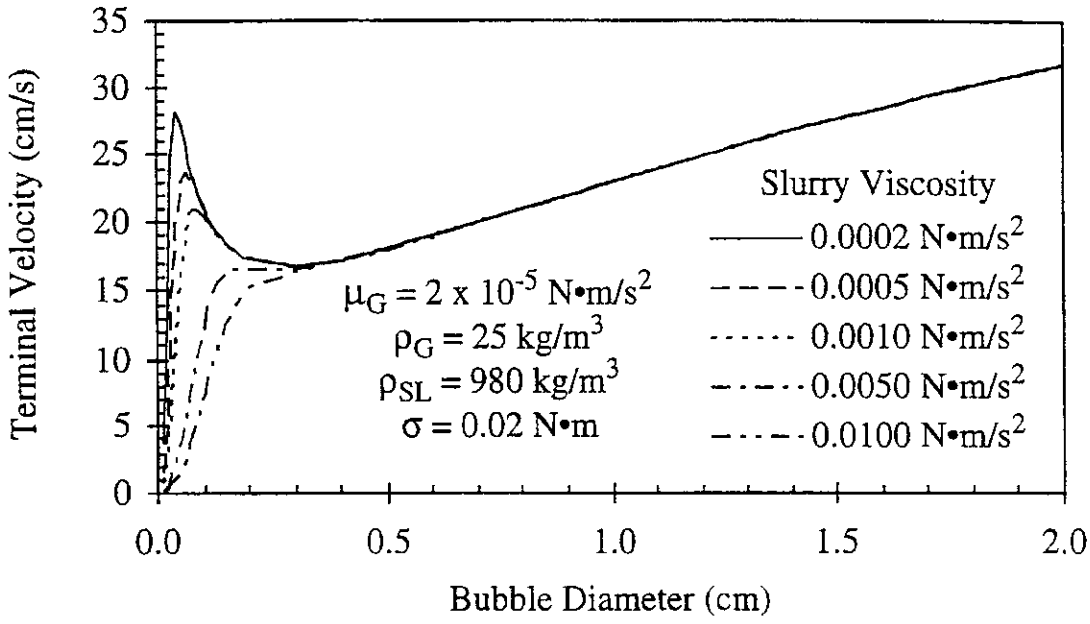

Figure 26. Terminal bubble velocity versus bubble diameter and liquid viscosity using correlation by Jamialahmadi (1994).

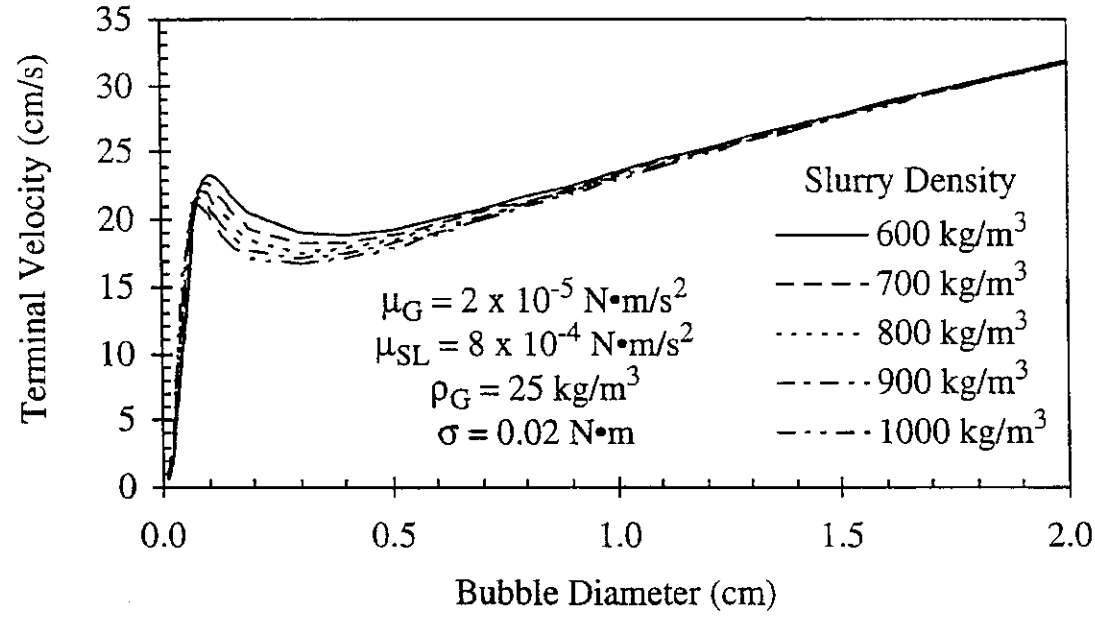

Figure 27. Terminal bubble velocity versus bubble diameter and liquid density using correlation by Jamialahmadi (1994).

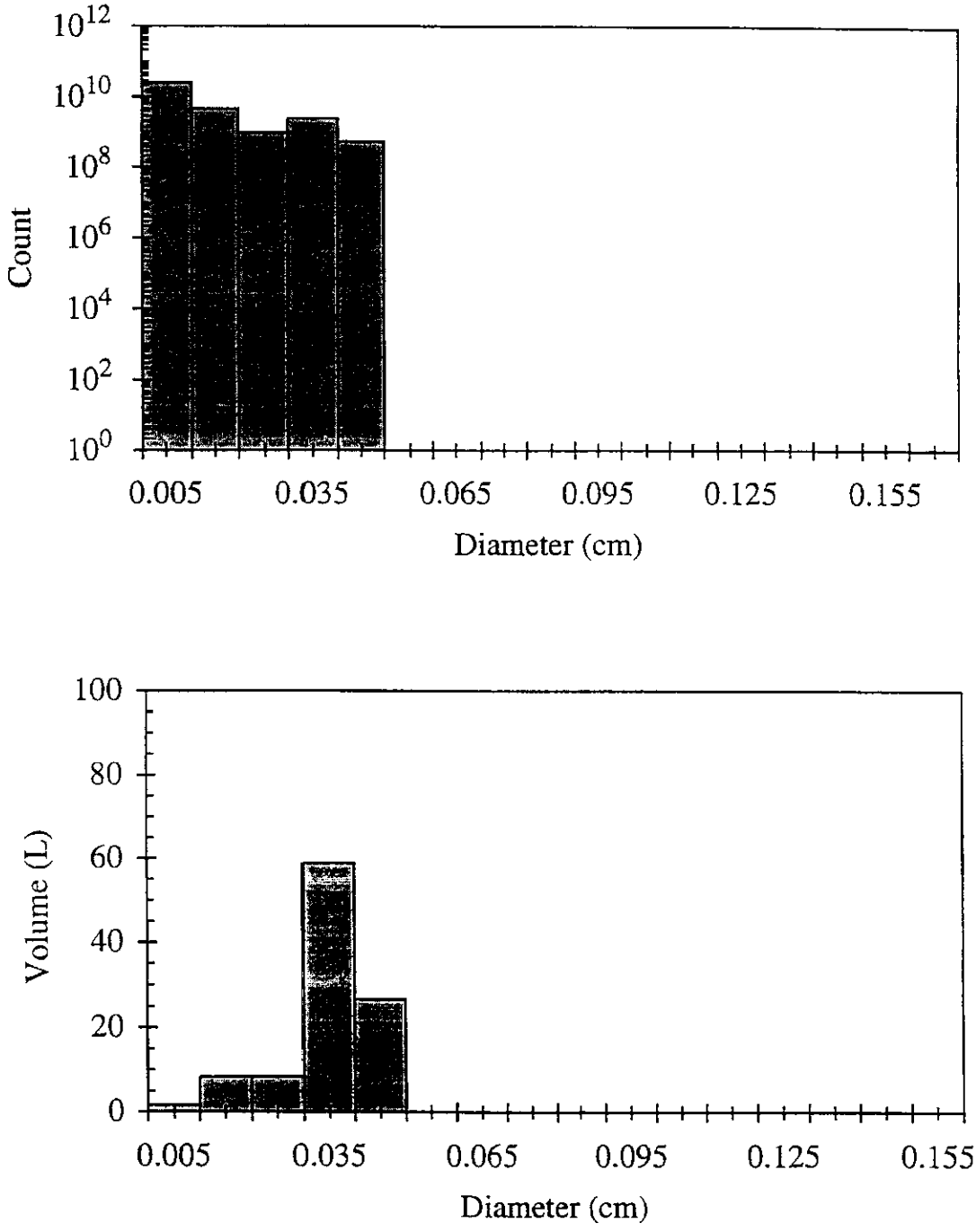

Figure 28. Number density and bubble volume histograms from DGD analysis and differential pressure measurements in AFDU for Run No. R13.2; $U_G = 0.15$ m/s, Kingsport gas, $\omega_S = 43\%$, catalyst A, 750 psia (5.17 MPa) and 482 °F (250 °C).

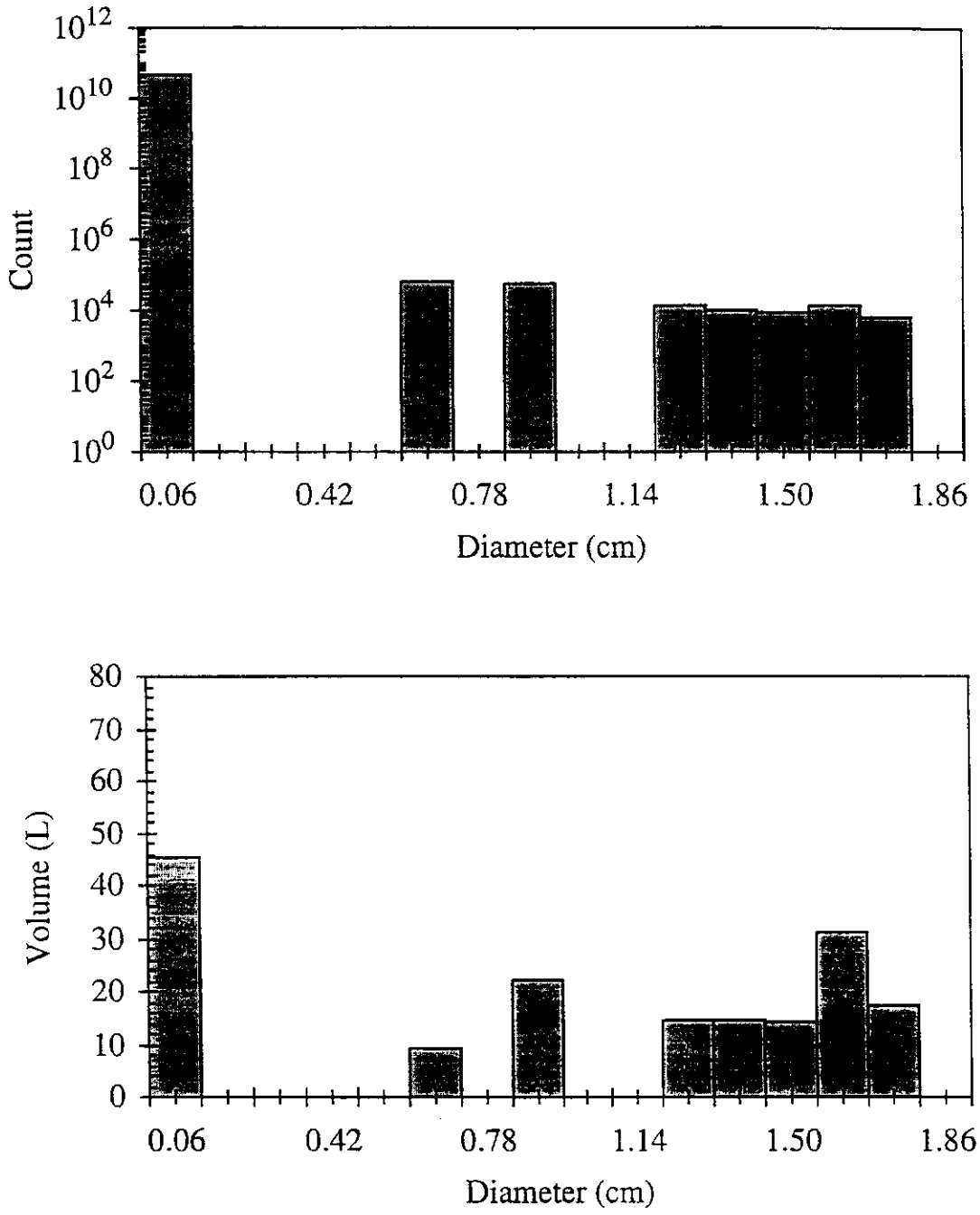

Figure 29. Number density and bubble volume histograms from DGD analysis and differential pressure measurements in AFDU for Run No. R14.1; U_G = 0.25 m/s, Texaco gas, ω_S = 43%, catalyst B, 750 psia (5.17 MPa) and 482 °F (250 °C).

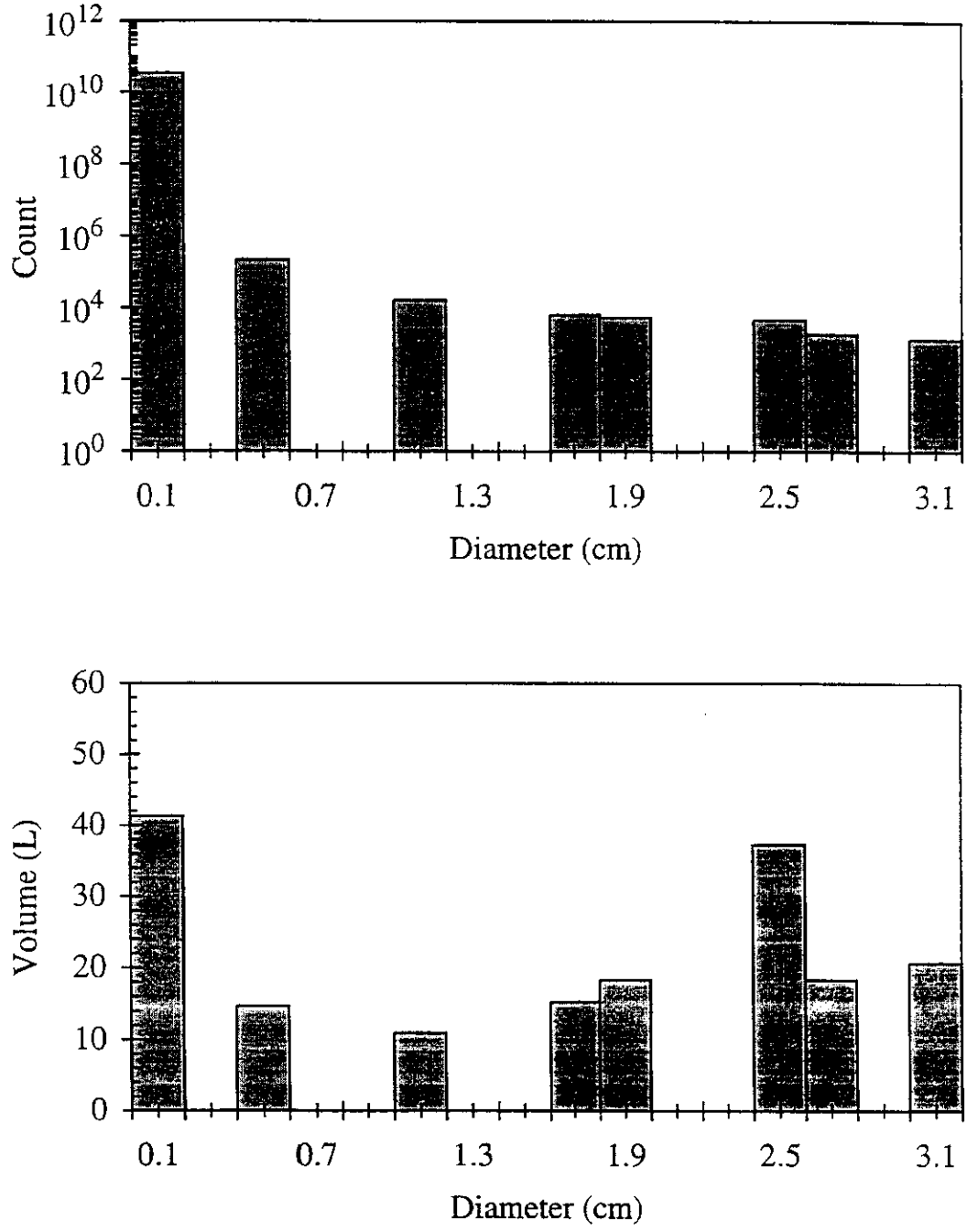

Figure 30. Number density and bubble volume histograms from DGD analysis and differential pressure measurements in AFDU for Run No. R14.3; U_G = 0.36 m/s, Kingsport gas, ω_S = 43%, catalyst B, 535 psia (3.69 MPa) and 482 °F (250 °C).